24th INTERNATIONAL CONGRESS ON SOUND AND VIBRATION
23–27 July 2017, London

ICSV24
23-27JULY 2017
LONDON CALLING

# A COMPUTATIONAL ANALYSIS OF SOUND DIRECTIVITY FROM SOUND PROPAGATION THROUGH NON-ISOTHERMAL, TURBULENT EXHAUST JETS IN CROSS-FLOW

Orddom Y. J. Leav, Benjamin S. Cazzolato and Carl Q. Howard
*The University of Adelaide, School of Mechanical Engineering, Adelaide, South Australia, Australia*
*email: orddom.leav@adelaide.edu.au*

When predicting community noise, it is commonly assumed that the directivity of sound from exhaust stacks is axisymmetric, which is appropriate in the absence of cross-flow. For real stacks, which typically carry hot exhaust gases this assumption is not valid. This paper analyses the effects of cooler cross-flow on the sound directivity of turbulent, heated, subsonic exhaust gas ejected from a stack. The analysis was first conducted using steady-state computational fluid dynamics to model the fluid dynamics associated with exhaust jets in cross-flow. The results of the computational fluid dynamics simulations, particularly the mean temperature and mean velocity components were then imported into a linearised Euler equation solver for conducting the sound propagation analysis. The flow conditions for this study were similar to conditions seen in large open-cycle gas-turbine exhaust-stacks, but scaled using non-dimensional acoustic and fluid dynamic parameters. The flow Mach number of the exhaust jet was approximately $0.1$ and a jet velocity to cross-flow velocity ratio of $5$ was chosen for analysis. Theoretically, an exhaust stack without flow would have spherical acoustic spreading at low frequencies at the duct outlet. However, the spreading is non-spherical due to the thermal gradient in the shear layer altering the propagation path of sound, as well as diffraction effects at the edge of the stack outlet. Furthermore, any cross-flow causes asymmetric spreading of the sound field. The computational results presented in this paper show that the presence of the turbulent non-isothermal, subsonic exhaust jet flow with cross-flow significantly alters the directivity of sound in the far-field (up to $3\,\mathrm{dB}$), thereby potentially impacting on nearby communities.

Keywords: Numerical sound propagation, exhaust jets in cross-flow, linearised Euler equations, computational fluid dynamics, sound directivity

## 1. Introduction

Open cycle gas turbines (OCGT) are increasingly been used for power generation as they are able to provide loads in peaking or uncertain conditions and can respond rapidly to power grid demands. However, there is considerable evidence suggesting that OCGT lead to higher noise levels than orthodoxy predicts [1, 2, 3, 4, 5]. This issue of low frequency gas turbine plant noise is almost entirely restricted to OCGT. Combined cycle gas turbines, which use the Brayton cycle and Rankin cycle, do not appear to suffer from the same issues. These excessive levels of low frequency noise from OCGT have caused documented detrimental effects to communities. The noise have previously lead to the following effects: perceived annoyance of ‘throbbing’ from high intensity low frequency noise [1], ‘beating’ sensation in the chest [6], nausea [1] and acoustic excitation in structures with low resonance frequencies, such as glass structures and wall panels [1].

Currently, the predicted sound levels from exhaust stacks is based on ISO 10494 [7] with a spherical source assumed at the exhaust stack outlet, and subsequent propagation predicted using ISO 9613 [8, 9]. However, in non-isothermal shear layers the propagation of sound can be altered due to the presence of velocity and temperature gradients in the shear layer [10, 11]. The study of shear layer sound refraction can be extended to the investigation of sound propagation through isothermal and non-isothermal jets, in which Atvars et al. [12] alluded that the non-isothermal jet shear layer can cause significant sound refraction. The refraction of sound due to the shear layer leads to the increase in off-axis SPL (sound pressure level) and a reduction in the on-axis SPL [12]. The effects of refraction are more pronounced with the increase in acoustic source frequency, thermal gradients from larger variations in jet temperature to ambient temperature, and velocity gradients from the increase in jet Mach number, $M_j$ [12]. Mungur et al. [13] has also shown with isothermal jets that the measurement location for the sound directivity is also important, as the jet shear layer developing downstream can cause sound refraction many diameters from the stack outlet.

The fluid dynamics associated with exhaust chimney stacks can be simplified to a flush mounted circular duct in a ground plane, which is known in literature as an elevated jet in cross-flow (EJICF) [14]. This particular type of flow configuration has been experimentally studied by various researchers [14, 15]. There are also different type of flow regimes with unique, time-averaged flow structures for EJICF and are governed by the jet to cross-flow momentum flux ratio [14] defined by: $R = \sqrt{\frac{\rho_j u_j^2}{\rho_{cf} u_{cf}^2}}$, where the jet velocity is $u_j$, the jet density is $\rho_j$, the free stream cross-flow velocity is $u_{cf}$, and the free stream cross-flow density is $\rho_{cf}$ [15]. Typically seen in OCGT are $R$ in the jet dominated flow regime for EJICF [14]. For this type of flow regime, unique flow structures that form include the following: deflected jet, jet shear layer, counter rotating vortex pairs, and stack shear layer [14].

Leav et al. [16] has conducted a previous study into sound propagation through a two-dimensional (2D) heated rectangular jet in cross-flow (JICF). It was observed in this numerical study that the thermal gradients associated with the JICF can lead to strong refraction effects downstream, which leads to asymmetric spreading on the leeward side of the duct and the formation of a highly directed lobe of sound. On the windward side of the duct however, the sound still spreads elliptically. ISO 10494 [7] is sufficient in predicting the sound power emitted, but not the directivity of sound. The study conducted by Leav et al. [16] had the following limitations: only the mean thermal gradient effects on sound propagation were analysed, the simulations were 2D, the duct was a rectangular piston, and the fluid dynamics are drastically different between 2D JICF compared to three-dimensional (3D) EJICF.

This paper analyses the effects that the steady-state, non-isothermal, exhaust jet with a cooler cross-flow has on the sound directivity. Computational fluid dynamics (CFD) and finite element modelling (FEM) are used for the analysis. The layout of the paper is as follows. The simplified computational model and boundary conditions of the computational mesh will be discussed in Section 2. Subsequently, the mathematical models that are used for the fluid flow simulations through CFD and acoustic propagation using linearised Euler equations (LEE) with FEM are explained. The simulation results from CFD and FEM are presented in Section 3, which shows the numerical fluid dynamics solution and the effects of the temperature distribution on the propagation of sound. The main conclusions of this paper are summarised in Section 4.

## 2. Details of computational models

### 2.1 Simplifications of the computational models and domain

The CFD and acoustic modelling of a real OCGT is a complex task, so consequently a simplified model of a JICF has been employed for this study. A schematic of the computational domain with the dimensions and corresponding boundary conditions can be seen in Figure 1. Only half of the domain is modelled in this particular simulation with a symmetry condition along the y-z plane. Not shown in Figure 1 is that the domain also spans $40D$ in the x-axis perpendicular to jet's symmetry plane

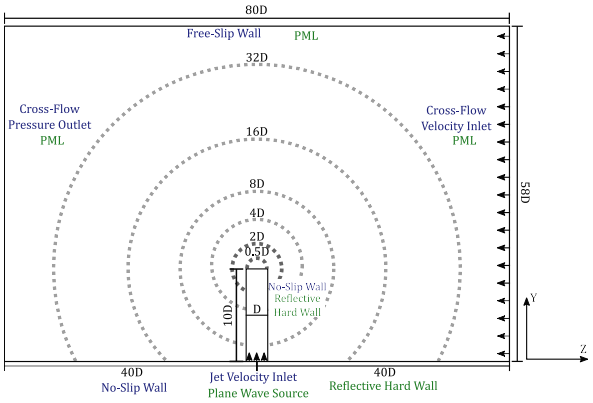


Figure 1: A schematic of the domain's geometry and boundary conditions, where $D$ is the duct inner diameter

(into the page). This truncation in the domain is possible due to previous literature indicating that the steady-state flow field is plane symmetric and preliminary acoustic simulation's showing that the sound field is also plane symmetric [15].

## 2.2 Boundary conditions

The correct use of boundary conditions are essential in resolving both the CFD and computational acoustic solution accurately. The boundary conditions for the simulation can be seen in Figure 1. The following assumptions have been made for the inlet boundary conditions for the 3D CFD simulation. The inlet conditions for the model are the turbulent, heated jet inlet at the base of the duct and the cross-flow on the windward side of the duct. For the jet inlet, a developed duct velocity profile with a bulk Reynolds Number, $Re_j$ of $38900$ was chosen. The fully developed duct velocity profile was achieved by first conducting simulations with a duct $40D$ long duct and the developed velocity profile at the duct outlet is interpolated onto the EJICF jet inlet. The $R$ chosen for this study is $5$. A constant mean velocity profile was applied to the inlet boundary. The resulting $M_j$ for this simulation is approximately $0.1$ and is typical of exhaust stacks. The jet inlet temperature was $773\,\mathrm{K}$, and resembles temperatures typically seen in OCGT exhaust stacks. The temperature at the cross-flow inlet was set to $300\,\mathrm{K}$. The duct walls and the ground wall adjacent to the circular stack are also no-slip walls.

In the far-field of the CFD model there are two different outlet conditions that are used. The outlet at the top of the domain in Figure 1 is a free-slip wall boundary condition. This was chosen to allow the shear stress along the wall to be set to zero. At the domain outlet, parallel to the cross-flow velocity inlet shown on the left in Figure 1 a pressure outlet condition is used.

In simulating the propagation of sound, two cases are considered here: with and without temperature distribution. The sound source was a planar harmonic source with a particle velocity amplitude of $0.5\,\mathrm{m\,s^{-1}}$. It is assumed in this study that the majority of sound is generated from primary the sound source (turbine) and other flow generated noise mechanisms can be neglected. This can be justified by the fact, that the quadrupole terms from shear layer noise are dependent on $M_{jet}^5$, which is almost negligible for the Mach number in this study. A Helmholtz number, $ka = 0.6$, where $k$ is the acoustic wave number based on the speed of sound, and a is inner radius of th duct, was chosen as it is a high enough such that it is comparable to the simulated plume's shear layer in Section 3.2.1 and is well below the cut-on frequency of the duct. Additionally, this was the highest $ka$ that can be simulated with the computational resources available and ideally a higher $ka$ closer to one would be better, at which the wavelength of sound would be small enough to interact with the shear layer.

For the computational sound propagation simulation, the far-field condition is uniform for all

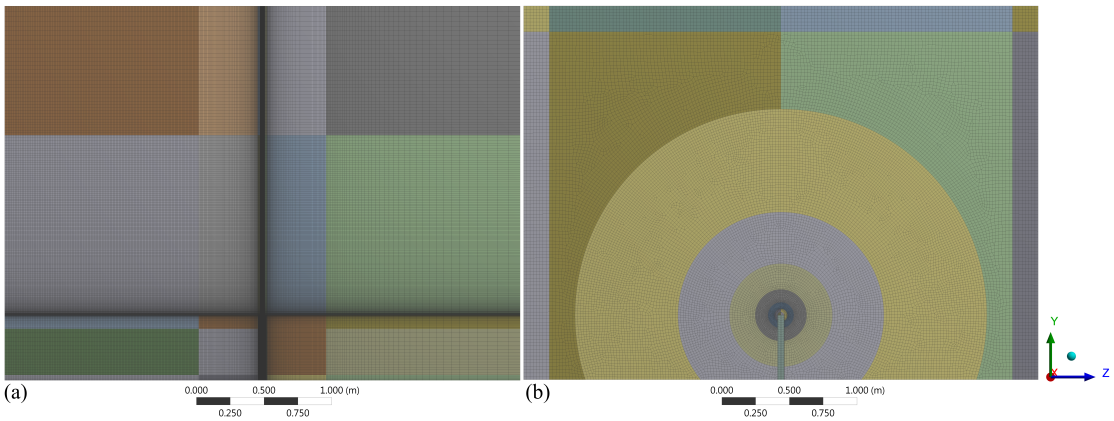


Figure 2: Non-isothermal EJICF mesh for CFD modelling (a) and mesh for LEE modelling with FEM (b)

boundary conditions. Perfectly matching layer (PML) elements are used for the far-field absorption of sound to simulate the free-field radiating condition. The number of PML elements used is dependent on the duct width, $D$, and the wavelength of sound. Howard and Cazzolato [17] have recommended that the PML zone is at least one-quarter of the wavelength wave length of sound.

## 2.3 Meshing details

For the CFD simulation the fluid dynamics were resolved using a mesh (shown in Figure 2) with structured hexahedra elements. Refinements were made in regions necessary for adequately resolving the critical flow features. This mesh has $15,250,000$ elements and $15,480,000$ nodes. The non-dimensional wall distance, $y^+$, for this simulation is more than 13, which is acceptable for resolving the boundary layer with the scalable wall function. In the geometric far-field where the flow characteristics are of less importance the mesh has been generated elements with high aspect ratio. The element type used in ANSYS FLUENT only specify nodes at the vertex of the element and is also known as 'brick' elements [18].

Mesh generation for modelling sound propagation with FEM has different requirements compared to the CFD simulation. The FEM mesh is shown in Figure 2. In propagating acoustic waves it is desirable to use a uniform mesh with minimal spatial changes in element size as it can cause numerical artefacts to form due to the minor impedance change, from different element sizes [17]. According to Howard and Cazzolato [17], at least six elements per wavelength are required for accurately resolving the acoustic pressure wave. Therefore, for the mesh shown in Figure 2 the $ka$ achievable for this simulation is $0.6$. The resulting acoustic element count is $1,280,000$ and node count is $4,850,000$. The mesh employs well defined arcs for ease of data post processing sound directivity at the radii of interest, structured hexahedra elements in the PML for the most effective attenuation of sound in the simulation [17].

## 2.4 Mathematical models

The fluid dynamics of the non-isothermal jet in cross-flow was simulated using ANSYS FLUENT [18]. The fluid flow in the model was computationally resolved using the compressible steady Reynolds Averaged Navier Stokes Equation (RANS). The fluid medium for this analysis is dry air. The density for the simulation was resolved using the ideal gas assumption. The viscosity of the model was calculated using the Sutherland approximation. A pressure based solver with a 'Coupled' setting for the pressure-velocity coupling was chosen. The spatial, pressure, energy and turbulent discretisation schemes chosen were a second-order upwind scheme. The two equation realisable $\kappa - \epsilon$

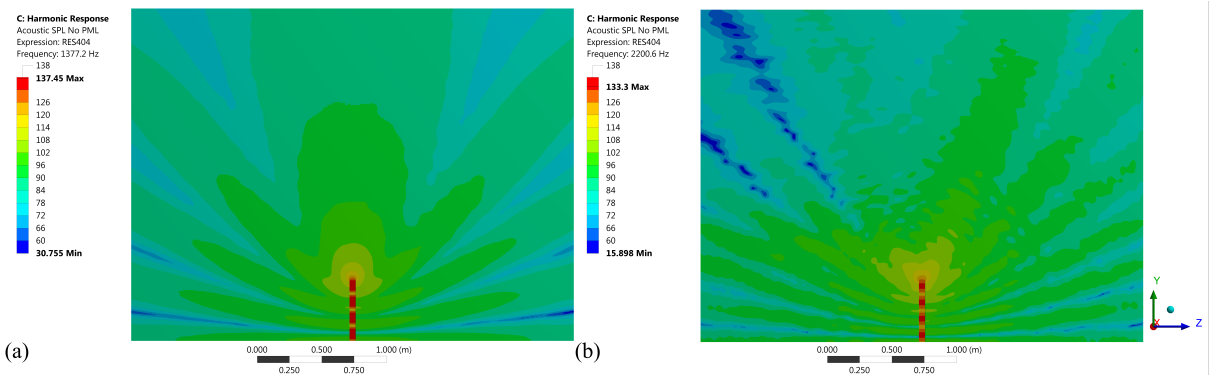


Figure 3: Acoustic SPL contour plot in a homogeneous medium (a) and in a media with temperature changes (b) along the y-z plane

model was chosen to resolve the turbulence [19]. This model is computationally less expensive than other more complicated RANS models and transient scale resolving turbulence models. However, there are limitations in the turbulence model: it assumes the eddy viscosity is isotropic; the turbulence can be modelled with two equations; the eddies in the models are not resolved with the average turbulence quantities being calculated in the shear layer; lack of prediction for flow separation at the jet inlet edge; and inaccurate prediction of the jet spreading and decay [19]. The boundary layer from the no-slip walls in the model were resolved using scalable wall functions. For the CFD analysis in this paper, only the critical steady-state features of the flow will need to be reproduced and the compressible steady RANS model is sufficient.

Sound propagation simulations were conducted by solving the LEE with FEM in ANSYS Mechanical with the Acoustic ACT extension [18]. In solving the LEE the following assumptions are made: the air medium is compressible, the changes in density are small in comparison to the mean density, the viscous dissipation of the fluid is neglected and the acoustic pressure can be represented by the wave equation. Harmonic analyses were chosen for this modelling work, as it allows the system to be driven by a sinusoidal oscillating harmonic source. The effect of temperature on propagation is modelled, however, the convective effects have been neglected as they have only minimal impact on refraction [16].

## 3. Computational Results

### 3.1 Absence of flow sound propagation

The sound propagating through the exhaust stack in the absence of mean flow was used as a benchmark case. The results indicate that in the absence of the heated mean flow, the acoustic spreading from the duct outlet is axisymmetric, as shown in Figure 3. However, due to the ground and duct walls being hard reflective surfaces there are reflections that propagate back into the domain and cause an increase in the SPL in the region below the duct outlet. This is to be expected when $ka$ is significantly less than one and the frequency of the harmonic planar source is less than cut-on frequency of the duct. The computational acoustic power results in the far-field ($32D$) have also been compared with the acoustic power results from the methods used in the ISO $10494$ [7], both were found to be $180\,\mathrm{dB}$ ref $10^{-12}$ W. Since, there is no difference it can be concluded that the standards are adequate in estimating the sound power from exhaust stacks without heated flow. However, it can be seen in Figure 3 that the radiation pattern is complex with the formation of pressure nodes. It can be observed in Figure 3, that the duct wall and the ground are causing the sound to reflect back into the domain. Hence, the spherical spreading assumption from ISO $9613$ [8, 9] does not hold for this particular scenario, as the radiation pattern is now complex.

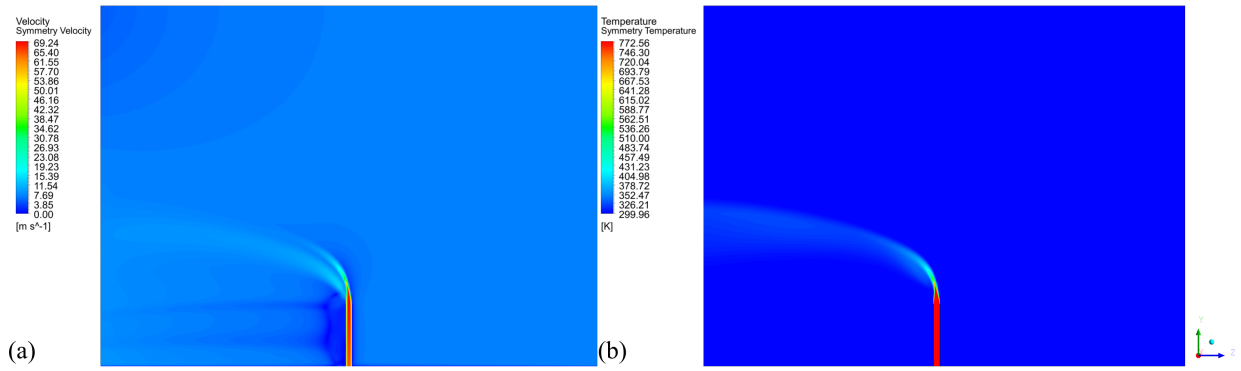


Figure 4: Velocity magnitude (a) and temperature (b) contour plots from modelling non-isothermal EJICF along the y-z plane, with the cross-flow from right to left

## 3.2 Non-isothermal elevated jet in cross-flow

### *3.2.1 Fluid features of non-isothermal elevated jets in cross-flow*

It can be seen in Figure 4 that the fluid issued from the duct outlet initiates as a jet in the geometric near field. As the jet fluid propagates downstream the jet begins to deflect due to the presence of the cross-flow momentum. The deflected plume transitions from a jet to a counter rotating vortex. The counter rotating vortex further develops and forms, as the dominant vortical structure in the plume downstream. During the formation of the counter rotating vortex, fluid is entrained from both the cooler cross-flow and the wake behind the stack in the simulation. A shear layer is also formed on the leeward side of the stack, which is due to the stack acting as a bluff body.

Figure 4 shows the temperature contour plot for the EJICF in the y-z plane. It can be seen that at the geometric near field close to the duct outlet the temperature profile resembles a jet, with the hottest region residing in the jet potential core. As the jet propagates downstream the plume is deflected by the cooler cross-flow stream's momentum and enhanced mixing occurs. This mixing causes lower temperatures seen in the plume's thermal gradients as the plume develops downstream. As the plume propagates downstream the plume's development into a counter rotating vortex then enhances mixing with the cooler cross-flow and reduces the temperature in the plume. The hottest region in the plume is the centre of the counter rotating vortex. This development of the plume has lead to the formation of thermal gradients where refraction of sound can occur. The effect of the thermal gradient on sound refraction is investigated in the following section.

### *3.2.2 Sound directivity of non-isothermal jets in cross-flow*

The steady-state, thermal distribution from the CFD simulation in Section 3.2.1 has been imported into the finite element model for sound propagation. The resulting SPL contour plot along the y-z plane is shown in Figure 4. In contrast to the case with a homogeneous media, the presence of the temperature distribution has drastically altered the propagation sound. Figure 3.1 shows that the sound radiation is no longer axisymmetric. There are now a distinct shift in lobes upstream and downstream, as well as the formation of a sound pressure null at $42\,\mathrm{deg}$. On the windward side, there is little changes to the acoustic radiation pattern and the spreading resembles the case in Section 3.1, which is to be expected as there are no significant fluid mechanic mechanisms that will change the sound propagation path. The lobes on the leeward side of the exhaust stack now differ from the previous lobes, concentrated closer towards the ground level of the domain. This change in acoustic radiation is a result of the thermal gradients associated with plume causing the sound to refract downstream and closer towards the ground. The sound power based on ISO $10494$ [7] in the geometric near field has been calculated and compared with the sound power in the far-field. The sound power based on

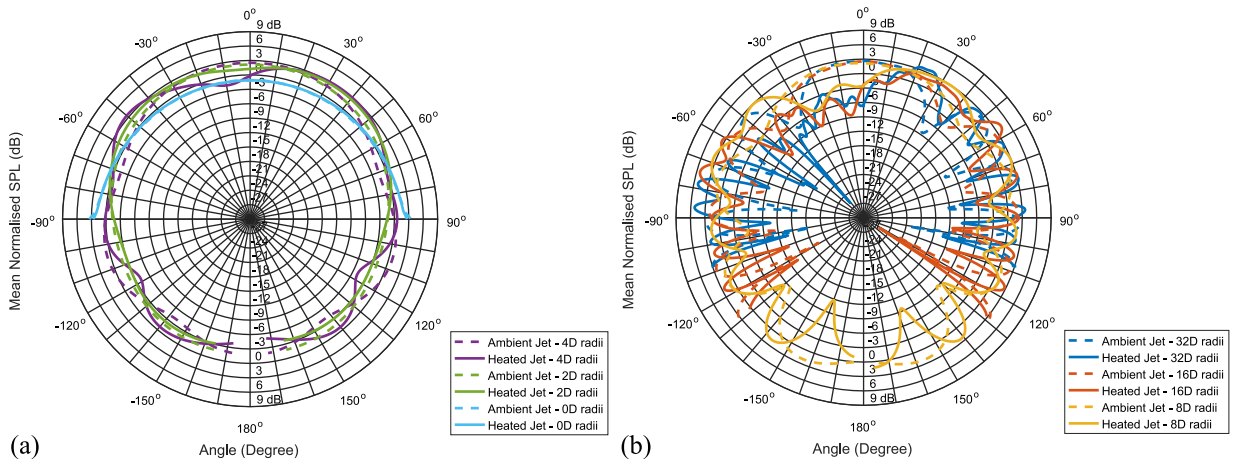


Figure 5: Mean normalised acoustic SPL directivity plots with varying radii from modelling with the EJICF thermal gradient's

the standards and far-field numerical measurements are both $180\,\mathrm{dB}$ ref $10^{-12}\mathrm{W}$.

In order to quantify the effects of refraction on the propagation path of sound, normalised SPL polar plots at varying spatial locations from the jet outlet were calculated and are shown in Figure 5. The results in each of the directivity plots are normalised with the mean SPL along the sphere with the same radii. Figure 5 indicates that at $0.5D$ there are edge diffraction effects due to the exhaust stack edge. For the sound directivity at the $2D$ and $4D$ arcs the acoustic spreading is almost spherical. This is the case as the plume's shear layer has yet grown spatially large enough for sound refraction. Figure 5 shows that as the arcs for sound directivity measurements increase in radii the sound becomes more directed downstream, with the magnitude in the lobe increasing by up to $3\,\mathrm{dB}$. This change in leeward side directivity is a result of the sound refraction becoming more prominent with the spatial growth in the non-isothermal shear layer. From the normalised SPL polar plots it can be seen that the EJICF has significantly altered the sound propagation path and the results are strongly dependent on the radial location for measurements, which is consistent with previous studies on sound propagation through unheated axisymmetric jets [13]. It was seen in early 2D studies [16], that further growth in SPLs along the horizontal can be expected at distances greater than investigated here.

## 4. Conclusion

The results from this study has shown that the thermal gradients in the plume from EJICF can affect the directivity of sound. The results have clearly indicated that in the absence of heated mean flow and without cross-flow, the propagation of sound from the duct is axisymmetric. However, this is not the case with the temperature distribution from the JICF, where the sound propagation is now asymmetric due to the sound refraction by the thermal gradients in the shear layer. Further analysis has shown the normalised SPL is strongly dependant on the radial location of the measurements. Even though the standards are sufficient in calculating the total acoustic power of the system in the far-field, the altered directivity of the 3D EJICF has shown that off-axis sound may be under predicted in the far field. The implications of these findings suggest that community noise levels from stacks may be under-predicted using ISO $9613$ [8, 9] due to the altered directivity of sound from the exhaust stack.

## REFERENCES

1. Broner, N. A simple outdoor criterion for assessment of low frequency noise emission, *Acoustics Australia*. **29** 1, 7–14, (2011).

2. Broner, N. Power to the people, *15$^{th}$ International Meeting on Low Frequency Noise & Vibration & its Control*, Stratford upon Avon, United Kingdom, 22–24 May, (2012).

3. Hessler Jr, G. F. Proposed criteria for low frequency industrial noise in residential communities, *Low Frequency Noise, Vibration and Active Control*, **52** 4, 179–185, (2004).

4. Hetzel, R. and Putnam, R. A. Sources and rating criteria of low frequency gas turbine exhaust noise - via case study, *INTER-NOISE and NOISE-CON, Congress and Conference Proceeding, 2009*, (2009).

5. Kudernatsch, G. Sources and rating criteria of low frequency gas turbine exhaust noise - via case study, *INTER-NOISE 2000, The 29$^{th}$ International Congress and Exhibition on Noise Control Engineering*, (2000).

6. Broner, N. The effects of low frequency noise on people - a review, *Journal of Sound and Vibration*, **58** 4, 483–500, (1978).

7. International Organization for Standardization. ISO 10494:1993 Gas turbines and turbine sets- Measurement of emitted airborne noise – Engineering survey method, *International Organization for Standardization*, Geneva, Switzerland, (1993).

8. International Organization for Standardization. ISO 9613-1:1993 Acoustics - Attenuation of sound during propagation outdoors – Part 1: Calculation of the absorption by the atmosphere, *International Organization for Standardization*, Geneva, Switzerland, (1993).

9. International Organization for Standardization. ISO 9613-2:1996 Acoustics - Attenuation of sound during propagation outdoors – Part 2: General method of calculation, *International Organization for Standardization*, Geneva, Switzerland, (1996).

10. Amiet, R. K. Refraction of sound by a shear layer, *Journal of Sound and Vibration*, **58** 4, 467–482, (1978).

11. Candel, S. M. Acoustic transmission and reflection by a shear layer discontinuity separating hot and cold regions, *Journal of Sound and Vibration*, **24** 1, 87–91, (1972).

12. Atvars, J., Schubert. L. K., and Ribner, H. S. Refraction of sound from a point source placed in an air jet, *American Institute of Aeronautics and Astronautics 2$^{nd}$ Aerospace Sciences Meeting*, (1965).

13. Mungur, P., Plumblee, H. E. and Doak, P. E. Analysis of acoustic radiation in a jet flow environment, *Journal of Sound and Vibration*, **36** 1, 21–52, (1974).

14. Adaramola, M. S., Sumner, D., and Bergstrom, D. J. Effect of velocity ratio on the streamwise vortex structures in the wake of a stack, *Journal of Fluids and Structures*, **26** 1, pp. 1–18, (2010).

15. Johnson, B. E. Elliot, G. E. and Christensen, K. T. Structural characteristics of a heated jet in cross-flow emanating from a raised, circular stack, *Experiments in Fluids*, **54** 6, 1543–1560, (2013).

16. Leav, O. Y. Cazzolato, B. S. and Howard, C. Q. Directivity analysis of sound in turbulent exhaust jets with laminar cross-flow: A numerical study. *Acoustics 2015 Hunter Valley*, (2015).

17. Howard, C. Q. and Cazzolato, B. S. *Acoustic analysis using MATLAB and ANSYS*, CRC Press, Boca Raton, Florida (2014).

18. ANSYS, *ANSYS Workbench 17.2*, ANSYS Inc, Canonsburg, Pennsylvania, (2016).

19. Shih, T-H., Liou, W. W., Shabbir, A., Yang, Z. and Zhu, J. A new $\kappa$–$\epsilon$ eddy viscosity model for high Reynolds number turbulent flows, *Computer & Fluids*, **24** 6, 227–238, (1995).